

Quantification of Inositol Hexa-Kis Phosphate in Environmental Samples

Lynne P. Heighton¹, Merle Zimmerman¹, Clifford P. Rice², Eton E. Codling², John A. Tossell^{1,3},
Walter F. Schmidt²

¹Department of Chemistry and Biochemistry, University of Maryland, College Park, USA; ²EMBUL ARS, USDA, Beltsville, USA;

³George Washington University, Department of Chemistry, Ashburn, USA.

Email: schmidt@ba.ars.usda.gov

Received January 14th, 2012; revised January 19th, 2012; accepted January 31st, 2012

ABSTRACT

Phosphorous (P) is a major contributor to eutrophication of surface waters, yet a complete understanding of the P cycle remains elusive. Inositol hexa-kis phosphate (IHP) is the primary form of organic (P_O) in the environment and has been implicated as an important sink in aquatic and terrestrial samples. IHP readily forms complexes in the environment due to the 12 acidic sites on the molecule. Quantification of IHP in environmental samples has typically relied on harsh extraction methods that limit understanding of IHP interactions with potential soil and aquatic complexation partners. The ability to quantify IHP *in-situ* at the pH of existing soils provides direct access to the role of IHP in the P cycle. Since it is itself a buffer, adjusting the pH correspondingly alters charged species of IHP present in soil. Density Functional Theory (DFT) calculations support the charged species assignments made based pK_as associated with the IHP molecule. Raman spectroscopy was used to generate pH dependent spectra of inorganic (P_I) and IHP as well as (P_O) from IHP and (P_I) in soil samples. Electro-spray ionization mass spectroscopy (ESI-MS) was used to quantify IHP-Iron complexes in two soil samples using a neutral aqueous extraction.

Keywords: Phytic Acid; Inositol Hexkis Phosphate; Electrospray Mass Spectroscopy (ESI-MS); Density Functional Theory (DFT); Raman Spectroscopy

1. Introduction

Increasingly it is understood that organic phosphorus (P_O) impacts environmental processes to a greater degree than has historically been given credence which has resulted in a lack of understanding of P_O fate and transport when compared to inorganic phosphate (P_I) [1-5]. Inositol phosphates specifically myo-inositol hex-kis phosphate (IHP) or phytic acid is the most prevalent form of P_O in soil systems [6-9]. Phytate anions and inorganic phosphate form complexes with metal cations that impact bioavailability of P and other trace nutrients in plants [10-13]. Negative impact occurs to open waterways from excessive loading of P from agricultural land resulting in the subsequent eutrophication. This process, as well as the inability to trace biological conversion processes to and from P_I to P_O in terrestrial and aquatic environments, could be better understood and thereby impacted by the identification and quantification of IHP and the metal-IHP complexes [1,4,14]. IHP has been implicated both positively and negatively in nutritional studies due to its ability to complex metals and the inability of many animal species to access the phosphorus from IHP [4,14-16]. The disso-

ciation of phytic acid results in acidic protons and a corresponding conjugate base. Each of the six phosphate groups has two acidic protons disassociating from the phytate anion at progressively higher pH and charge [10,11]. At the molecular level, it is ambiguous whether some, all or none of the six acidic sites have specific pK_a values, *i.e.* are equally acidic. Raman spectra of IHP have been shown to differ with pH. This is consistent with the non-equivalence among acidic P sites on IHP. Computational chemistry using Density Functional Theory (DFT) has been successfully used to characterize physical properties of chemical structures from quantum mechanical principles and could provide a molecular basis for characterizing the relative acidity of the IHP phosphate groups [17].

Electro-spray ionization (ESI-MS) provides a unique and precise method to investigate the parent ions of phytate and phytate-cation complexes at multiple pH values [18]. The procedure provides useful information about phytate speciation in more complicated matrixes, as well as in obtaining association constants required for modeling the fate of P_O in complex environmental systems. More broadly, adding multivalent cations (or anions) to

the mobile phase in ESI-MS can assist in identifying previously unassigned fragments from multi-charged anionic (or cationic) species. As cations of iron are the most abundant metal in soil systems, Fe^{+3} (and Fe^{+2}) is (are) the clear choice for investigation of *in-situ* IHP-metal complexes.

2. Materials and Methods

Soil Sample History. Two Maryland soils, Matapeake silt loam (B) and Evesboro sand (Q) were collected in 2000 for a previous publication and amended at that time with 0.5% iron in order to determine the benefit of iron in phosphate sequestration. The soils were analyzed for carbon content, water Soluble P (mg/Kg), Bray & Kuntz soil test (g/Kg), pH and organic C (g/Kg) as described previously in Codling *et al.* 2000 [19]. The soil samples were obtained from agricultural fields that have a thirty year history of fertilization with poultry litter. Both soils were known to be high in total P. The results of the soil analyses from the original paper are summarized in **Table 1**. The soil and iron amendment were stored at room temperature, in the dark for 10 years before use in this study.

Electrospray-Ionization Spectroscopy. Phytic acid dodecasodium salt (IHP) ($\text{C}_6\text{H}_6\text{Na}_{12}\text{O}_{24}\text{P}_6$), with a formula weight of 798 purchased from Sigma Chemical (St. Louis, MO) (Sigma P8810) and Iron (3) chloride hexahydrate ($\text{FeCl}_3 \cdot 6\text{H}_2\text{O}$) supplied from Sigma Aldrich Chemical (St. Louis, MO) were used to prepare fractional species of iron adducts of IHP at pH 6 in a ratio of 1.5 mM IHP to 3.0 mM ferric chloride (Fisher Scientific). The fractional species of phytate (α) derived from pKa of IHP, as well as the (α) of selected metal adducts of IHP were previously reported in Heighton *et al.*, 2008 [11]. Iron complexes of IHP were investigated using a Waters Quattro LC with Mass Lynx software. Instrumental parameters such as cone and capillary voltage were adjusted to achieve robust spectra. In this case the capillary voltage was 3.05 kV and cone voltage was 63 V and the spectra were collected in electrospray negative acquisition mode using scan ranges from 180 to 206 m/z . Samples and standards

were introduced by direct injection of 10 μl loop additions to the mobile phase (1% formic acid: methanol) (70:30) flowing into the electrospray interface at the rate of 0.3 ml/minute from a high pressure liquid chromatography pump (HPLC). The peak at 198 m/z was used to generate a standard curve with a correlation coefficient of 0.99 and a linear range of 0.005 - 0.05 ppb. Five replicates of each concentration were used to generate standard curves. Soil samples and 0.5% iron amended soil (1.0 g) described above were extracted with 10 ml of pH 6 reverse osmosis (RO) water for 12 and 24 hours using an end over end shaker, then centrifuged with a Beckman J2-M1 at 10,000 rpm for 15 minutes at 25°C. The samples were pH adjusted to pH 6.0 before and after extraction with concentrated hydrochloric acid (HCl) or concentrated sodium hydroxide (NaOH). The iron adducts of IHP were quantified using the 198 m/z standard curve.

In a second experiment ethylene diamine-tetraacetic acid (EDTA) ACS grade from Fisher Scientific with a concentration of 0.5 mM was added to the each soil and 0.5% iron amended soil and extracted in the same manner as the soil samples in the first experiment. These samples were also analyzed for the presence of the 198 m/z cluster of peaks.

Statistical Analysis. The program Sigma Plot 11.2 [20] was used to test for statistical differences in ESI-MS derived concentration of IHP. An ANOVA was used initially to test for Normality and Equal Variance in the control and 0.5% iron amended soils. The data did not meet the requirements for equal variance ($p < 0.050$) [20]. A Friedman Repeated Measures of Variance on Ranks with post hoc Tukey group pairings was used to test for statistically significant differences in IHP concentration among soils (Evesboro sand and Matapeake silt loam) and treatments (soil controls, 0.5% Fe amendment and EDTA extraction). Analyses were considered to be statistically significant at $p < 0.05$.

Raman Spectroscopy. A Horiba Jorbin Yvon LabRAM Raman Spectrophotometer equipped with a helium-neon laser (632.8 nm excitation line) and a 532 nm diode laser were used to measure the pH dependent Raman spectra of inorganic and organic phosphate standards and soil samples. Spectra were obtained using a 1 cm quartz cuvette or the confocal microscope in conjunction with borosilicate slides with aluminum backing, and a charged coupled detector cooled to -28°C . The instrument was calibrated using the 519 cm^{-1} line of silicon. Backscattered radiation was collected with the optical slit set to 100 μm and the pin hole set to 500 μm . The holographic grating was set to 1800 grooves/mm.

IHP was prepared at 100 mM and filtered with a 0.47 μm glass micro-fiber filter (934-AH) from Whatman. Aliquots of filtered phytic acid were pH adjusted with a minimal amount of concentrated hydrochloric acid or

Table 1. Soil analysis of two agricultural soils from Maryland.

Soil Analysis	Matapeake	Evesboro
Soil Texture	Silt Loam	Sand
Water Soluble P (mg/Kg)	41	84
Bray & Kuntz Soil Test (g/Kg)	1.26	0.96
pH	4.6	5.6
Organic C (g/Kg)	18	29

sodium hydroxide to pH's spanning pH 3.0 to pH 10.5 in 0.5 pH unit increments. Raman spectra were collected at each pH interval. Monosodium phosphate (monobasic) ($\text{NaH}_2\text{PO}_4 \cdot \text{H}_2\text{O}$) with a formula weight of 137.99 was obtained from J.T. Baker & Co. (Phillipsburg NJ) and sodium phosphate dibasic ($\text{Na}_2\text{HPO}_4 \cdot 2\text{H}_2\text{O}$) Reagent plus $\geq 99\%$ purity from Fisher Scientific were used to prepare 10.0 ml of inorganic phosphate buffer with a concentration of 600 mM at pH intervals of 0.5 pH units from pH 3.0 to pH 10.5. Raman spectra were collected at each pH interval. Concentration dependent spectra of phytic acid were collected at pH 4.5 and pH 7.0.

Raman spectroscopy was also used to identify inorganic and organic phosphate in the previous described soil samples (Matapeake and Evesboro) (**Table 1**) A series of spectra of each soil and each 0.5% iron amended soil were taken as a function of pH. The soils were spiked with either 100 mM of phytic acid or 600 mM of inorganic phosphate. The PA spiked soils were compared to ferric phytate slurry with a ratio of 300 mM Fe^{3+} to 100 mM IHP using an aluminum backed slide.

Theoretical Raman Spectra. Computational calculations were conducted in support of the experimental Raman spectra. The following calculations were used to explore the possible pH dependent spectral changes. As the IHP ($\text{C}_{12}\text{H}_6\text{P}_6\text{O}_{24}$, the 12 exchangeable protons are not included in the IHP designation) system was relatively large, we started with a Hartree Fock [21] calculation with a smaller basis set, 6-31G. B3LYP [22] calculations were performed on the same systems to confirm the stability of the HF spectral results. Calculations were conducted with Gaussian 03 [23]. The main three compounds which

we examined were H_{12}IHP (fully protonated), $\text{H}_6\text{IHP}^{6-}$ (half deprotonated), and IHP^{12-} (fully deprotonated). These three were chosen to cover the four main states of the phosphoric acid groups, fully protonated $[\text{H}_3\text{PO}_4]^0$, $[\text{H}_2\text{PO}_4]^-$, $[\text{HPO}_4]^{2-}$, and fully ionized $[\text{PO}_4]^{3-}$. As these particular species show the most differentiation in their experimental spectra as well as population in vivo systems, they should allow us to cast the most light on the experimental results. Initial calculations were gas phase only, followed by explicit hydration with 6 water molecules in each system. This was done successfully for $\text{H}_6\text{IHP}^{6-} \cdot 6\text{H}_2\text{O}$.

3. Results and Discussion

Experimental Raman Spectroscopy. The pH dependent Raman spectrum of P_i as orthophosphate (H_3PO_4) exhibits three titratable peaks between 800 and 1100 cm^{-1} (**Figure 1**).

These peaks changing as a function of pH can only be attributed to the molecular response to the protonation/deprotonation of orthophosphate as H_2PO_4^- is titrated to HPO_4^{2-} at pK_a_2 7.2. Two sharp peaks are apparent between pH 3.0 and pH 5.0 at Raman shifts of 867 and 1062 cm^{-1} . These two peaks disappear at pH 7.0 as a peak at Raman shift 976 cm^{-1} emerges at pH 5.0, growing to full intensity at pH 7. Another transition appears at pH 10 as the spectral peak at Raman shift 976 cm^{-1} decreases in intensity and a second Raman peak appears at spectral shift 921 cm^{-1} . This transition is likely associated with the loss of the HPO_4^- proton at pK_a_3 12.35 as HPO_4^- is titrated to PO_4^{3-} .

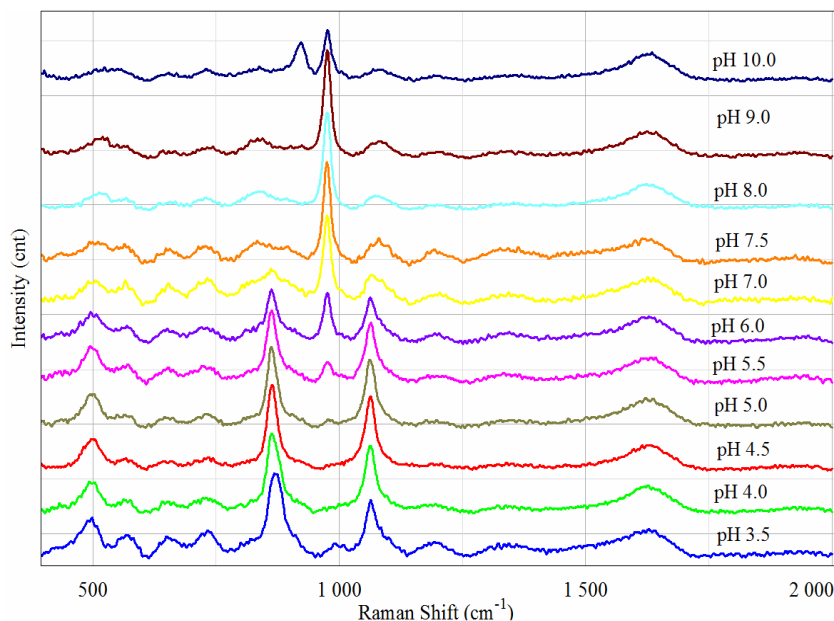


Figure 1. pH dependent Raman spectra of inorganic phosphate (P_i) as orthophosphate (600 mM) buffered, at pH from 3.5 to pH 10.

The pH dependent Raman spectra of P_O as IHP exhibits a similar pattern of peaks and response to titration as the P_I spectra between 800 and 1100 cm^{-1} , but differs from the P_I in several distinct ways (**Figure 2**). The first difference is that the P_I peak 863 cm^{-1} in the P_O spectra is shifted by 30 cm^{-1} to 832 cm^{-1} . The second difference is associated with the emergence of the peak at Raman shift 976 cm^{-1} which begins to appear in the IHP spectra at pH 6.5, much later than in the P_I spectra in which it appears at pH 5.0. Finally, the peak at 1062 cm^{-1} which disappears in the P_I Raman spectra at pH 7.0 never disappears in the P_O spectra indicating that is not associated with titratable protons but instead part of the carbon structure of IHP. This peak in the IHP spectra is broader and flatter than the equivalent peak in the orthophosphate (P_I) sample indicating two unresolved peaks in the IHP sample and only one peak in the P_I . This position is supported by the theoretical data and discussed later. Notably, the IHP spectra does not change substantially between pH 3.0 and pH 6.0 which is an indication of no or very small conformational changes in the molecule. The additional peaks in the Raman spectra of IHP are likely modes within the molecule that are unaffected by the titration of the phosphate groups on the molecule. The structure of IHP in the form of $\text{C}_6\text{H}_{18}\text{P}_6\text{O}_{24}$ (H_{12}IHP) was determined by is provided in **Figure 3**.

Raman spectroscopy can be used to differentiate P_I from P_O (as IHP) in standard solutions due to the differences in the pH dependent spectra of IHP and P_I (**Figure**

1 and **Figure 2**). The detection limits for normal Raman spectroscopy of P_I and IHP have high concentrations, rendering the technique of little use in environmental samples without a pre-concentration step (**Figure 4**).

Soil samples Matapeake silt loam and Evesboro sand were examined using Raman spectroscopy at pH 4.5 by Raman Spectroscopy and P_O was found to be indistinguishable from P_I using the current experimental conditions (**Figure 5**). Addition of Ferric cation was found to reduce the intensity of P_O as IHP and P_I in both soils. Clearly, P_O and P_I sites simultaneously compete for the same metal ions. At the molecular level, the specific sites $1P_O$, $2P_O$, $3P_O$, $4P_O$, $5P_O$ and $6P_O$ are not structurally equivalent so each of the twelve protons attached to the six P sites will not be identical in their ability to form H_3O^+ ions.

Raman Spectra Derived from Theoretical Calculations. Normal vibrational spectroscopy provides lower detection limits than gravimetric analysis does and greater specificity toward forms of P than colorimetric analyses does, but it does not provide enough sensitivity for development of *in-situ* probes, which is the ultimate goal of this work. A pre-concentration step is required to generate relevant environmental data from normal Raman spectroscopy. An alternative to pre-concentration is surface enhanced Raman spectroscopy. This method has the potential to provide the sensitivity needed for *in-situ* probes, while maintaining the ability to provide speciation of P in unaltered or minimally altered environmental samples.

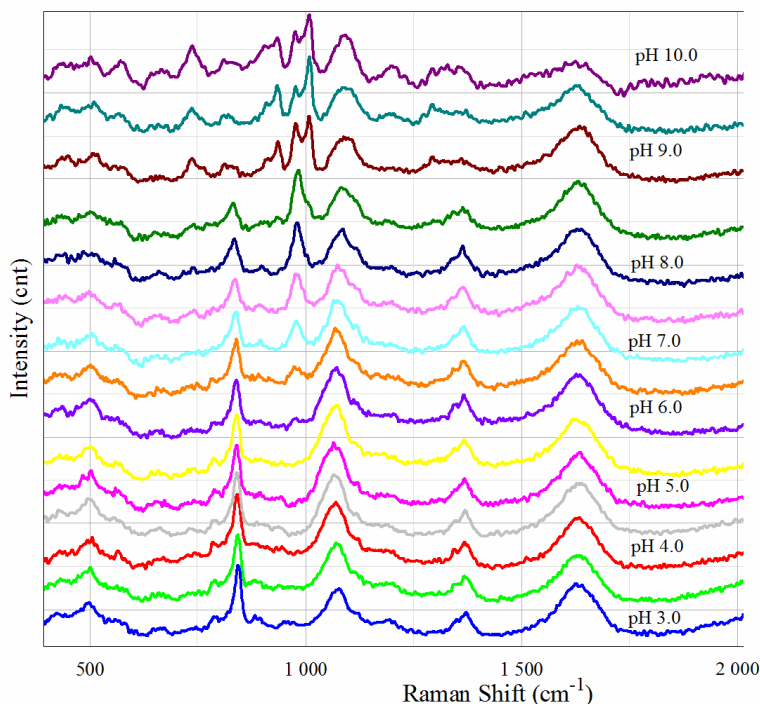


Figure 2. pH dependent Raman spectra of organic phosphate (P_O) as inositol hex-kis phosphate (IHP) (100 mM) at pH 3.0 to pH 10.

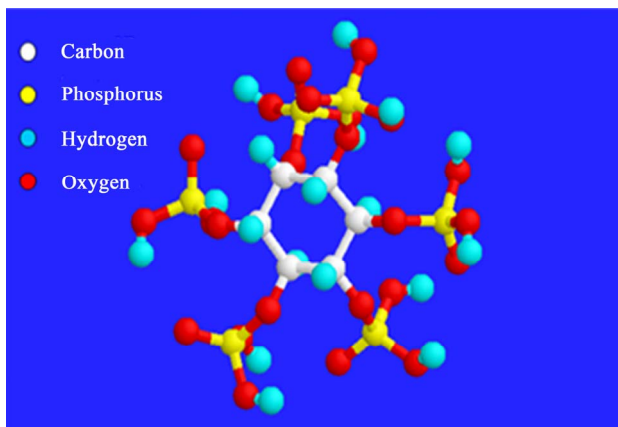


Figure 3. Structure of Inositol hex-kis phosphate (IHP) as $C_6H_{18}P_6O_{24}$ ($H_{18}IHP$).

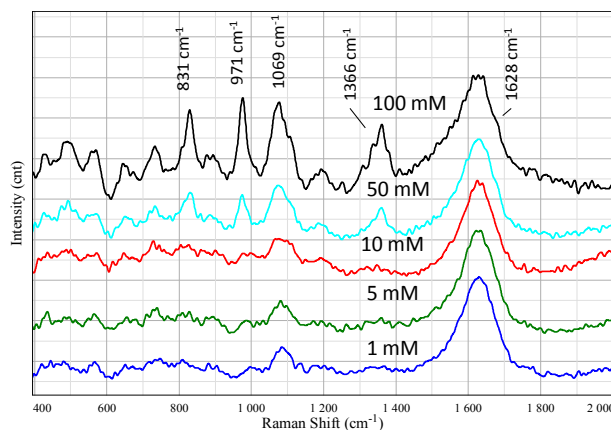


Figure 4. Raman intensity of organic phosphate (P_O) as IHP as a function of concentration (mM) at pH 7.

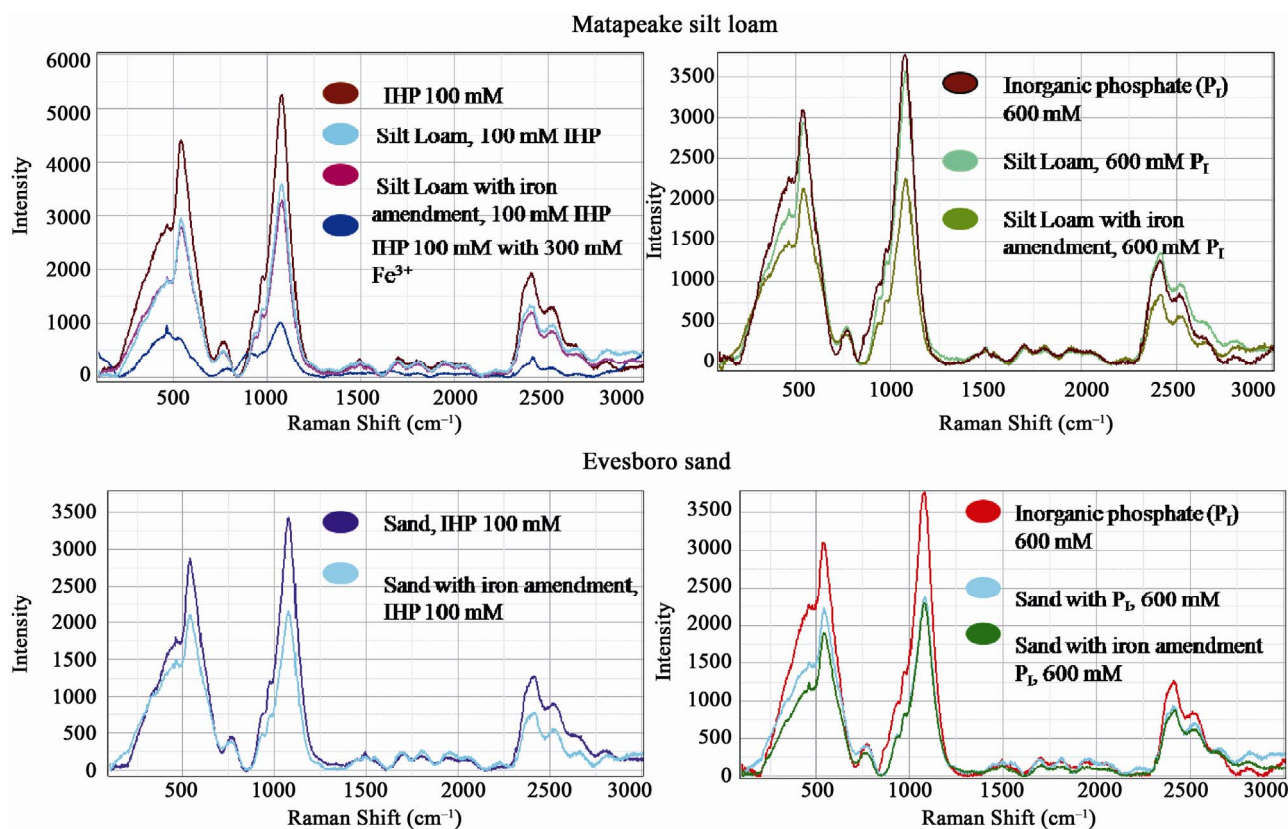


Figure 5. Raman spectra of two high phosphorous soils (pH 4.5). Soil control and 0.5% iron amended soils were spiked with IHP or orthophosphate.

The primary vibrational mode at 832 cm^{-1} is the hydrogen-bonding phosphate H atoms moving perpendicular to the axis of hydrogen bonding between adjacent phosphate groups. The primary mode at 967 cm^{-1} appears to be a symmetric stretch that appears when the phosphate is deprotonated, while the mode at 1100 cm^{-1} corresponds to an asymmetric stretch of the same groups. The peaks near 1500 appear to be H atom bending. The peaks around 1162 cm^{-1} correspond to various vibrational

modes of the C_6 ring in the center of the compound. We can now compare our Raman data to experimental spectra taken under various pH conditions, as shown in Figures 2-5. Looking between the peaks seen experimentally at low (acidic) pH 3, where the fully protonated $H_{12}IHP$ would be predominant, and the peaks seen in more neutral solutions near pH 7, we can first observe in the experimental data that there is a trend where the peak at 850 cm^{-1} shrinks, and a peak appears near 1000 cm^{-1} .

This trend is duplicated in our theoretical data for the explicitly solvated $\text{H}_6\text{IHP}^{-6}\cdot 6\text{H}_2\text{O}$ anion as calculated with the HF/6-31G.

The peak slightly below 1000 cm^{-1} in the experimental spectra is probably the phosphate symmetric stretching mode shown by the singly deprotonated $\text{HPO}_3\text{-R}$ groups in our calculation and shown in **Figures 2** and **4**. The peak further down is the vibrational modes of the intramolecularly hydrogen bonding protons on the phosphate groups vibrating perpendicular to the bonds. This would explain the near disappearance of the peak in the most basic conditions, where the acidic groups would be fully deprotonated and this kind of mode would no longer be possible. Finally, the peak just above 1000 cm^{-1} is related to the vibrational modes of the central C_6H_6 ring, it remains for the most part unchanged regardless of the external pH. The modes between 1450 and 1600 cm^{-1} on our spectrum appear to correspond to different bending modes of non-bonding H atoms, mostly on the central C_6 ring, although they also include some motion of phosphate H atoms in unfavorable directions. This might explain why the peaks seen on the experimental spectrum in this area become subdued under the most basic pH conditions.

The clear trends of where the Raman absorptions are with relation to each other correspond closely to the experimental results, confirming the identities of the species suspected by the experimenter. Theoretical vibrational modes provided additional insight into the sources of each observed peak in the experimental measurement.

Currently, further efforts continue to model the solvated, fully deprotonated IHP^{-12} system, and this additional information will be presented in a future paper. Future calculations on explicitly solvated molecules of the fully deprotonated IHP^{-12} should shed further light on the area of the experimental spectrum in the $1200 - 1700\text{ cm}^{-1}$ area as well, as changes were observed there compared to the H_{12}IHP and $\text{H}_6\text{IHP}^{-6}$ systems examined here.

Electrospray Ionization Spectroscopy. The speciation (α) of the IHP at pH 6 can be predicted from previously published pKa data [10,11,18] to be a distribution of 3 sequentially charged species: $\text{C}_6\text{H}_5\text{P}_6\text{O}_{24}^{-8}$ ($\text{H}_4\text{IHP}^{-8}$), $\text{C}_6\text{H}_5\text{P}_6\text{O}_{24}^{-7}$ ($\text{H}_5\text{IHP}^{-7}$) and $\text{C}_6\text{H}_5\text{P}_6\text{O}_{24}^{-6}$ ($\text{H}_6\text{IHP}^{-6}$). The majority (60%) of IHP at pH 6 is present as $\text{H}_5\text{IHP}^{-7}$. A mass spectral peak is expected to be present at m/z of 93. This peak represents $\text{H}_5\text{IHP}^{-7}$ with a mass of 653 amu and a $z = 7$. The m/z is present in standards, but is predictably not observed in natural samples due to the ability of IHP to form strong complexes with metals.

Iron (Fe^{3+}) complexes of IHP are readily formed and produce ESI-MS spectra that are predictable and quantifiable at ppb levels in standard solutions (**Figure 6**). The spectral peaks at m/z 196, 198 and 200 as well as the total ion count (TIC) over a range of $180 - 700\text{ m/z}$ were scrutinized for possible use in quantifying iron complexes in soil samples. The peak at 198 m/z (**Table 2**), (**Figure 6**) was used to identify iron complexes of IHP in two soil samples Matapeake silt loam and Evesboro sand (**Figure 7**).

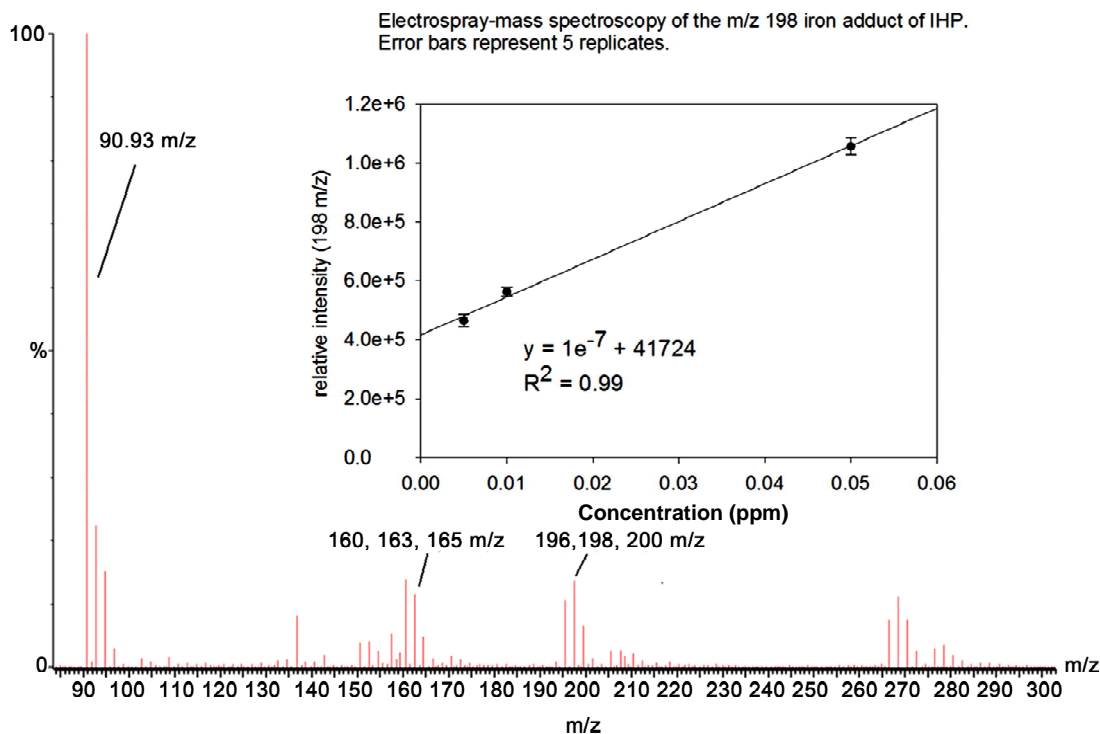
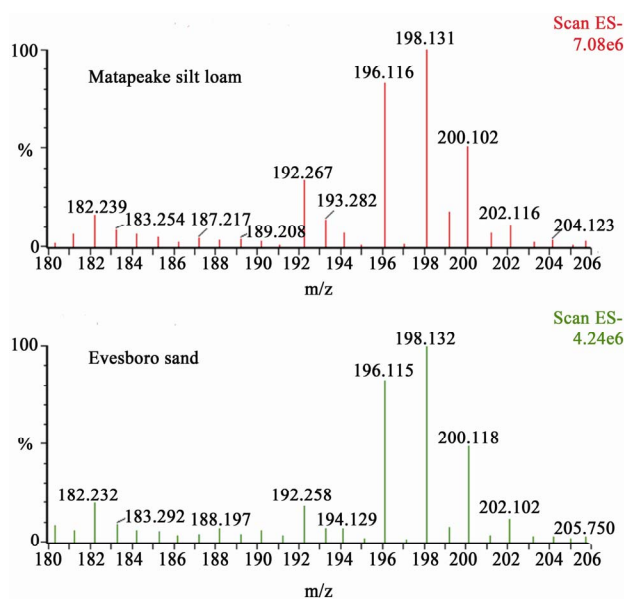


Figure 6. IHP-iron complex ESI-MS spectra. Standard curve at 198 m/z (inset).

Table 2. Phytic acid and ferric chloride at pH 6 ESI-MS peak assignments.

pH 6 Peak Assignment	z	m/z	m	Charge
$\text{Fe}^{56}\text{H}_2\text{O}_2$	-1	90	90	-1
$\text{C}_6\text{H}_{11}\text{O}_{24}\text{P}_6$	-7	93	653	-12 + 5
$\text{C}_6\text{H}_{12}\text{Fe}_5^{56}\text{O}_{36}\text{P}_6$	-7	160	1126	-12 + 15 - 10
$\text{C}_6\text{H}_{12}\text{Fe}_5^{56}\text{O}_{37}\text{P}_6$	-7	163	1142	-12 + 15 - 10
$\text{C}_6\text{H}_{12}\text{Fe}_5^{56}\text{O}_{38}\text{P}_6$	-7	165	1158	-12 + 15 - 10
$\text{C}_6\text{H}_{12}\text{Fe}_5^{56}\text{O}_{36}\text{P}_6 \cdot \text{Cl}$	-7	196	1126/7 + 35	-12 + 15 - 10
$\text{C}_6\text{H}_{12}\text{Fe}_5^{56}\text{O}_{37}\text{P}_6 \cdot \text{Cl}$	-7	198	1142/7 + 35	-12 + 15 - 10
$\text{C}_6\text{H}_{12}\text{Fe}_5^{56}\text{O}_{38}\text{P}_6 \cdot \text{Cl}$	-7	200	1158/7 + 35	-12 + 15 - 10

**Figure 7. ESI-mass spectra of Matapeake silt loam (upper spectra) and Evesboro sand (lower spectra).**

The concentration of IHP iron complexes quantified from the 198 m/z show statistically measureable differences between Evesboro sand (**Figure 8** Tukey group a) and Matapeake silt loam (**Figure 8** Tukey group b). No difference was found between the soil control and the 0.5% iron amendments for either soil (**Figure 8** Tukey groups a and b).

EDTA extractions of both soil controls and respective 0.5% iron amendments were found to be statistically different (**Figure 8** Tukey group c). Addition of EDTA to the soil samples was found to eliminate m/z peaks at 196, 198 and 200.

Interestingly, in the case of iron at pH 2.8 and 6 specific, consistent and repeatable clusters are formed regardless of the initial pH. Clusters centered at 163 and

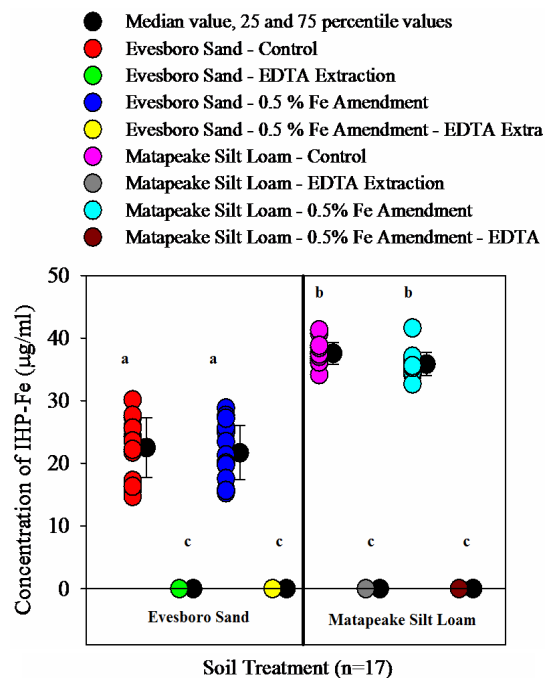


Figure 8. A Friedman Repeated Measures Analysis of Variance on Ranks with post hoc Tukey groupings (a, b and c) of Evesboro sand and Matapeake silt loam extracted with water at pH 6 or EDTA at pH 13 and monitored with the 198 m/z ESI-MS spectral peak found statistical differences between the median concentrations of Evesboro sand and Matapeake silt loam (Tukey groups a and b), but did not find statistical differences between the median concentrations of each soil and their respective 0.5% iron amendment. The median concentration values of the EDTA extractions were found to be statistically different in both controls and amendments of each soil (Tukey group c).

198 m/z are the dominate species in each spectra. The distribution of IHP charge speciation is expected to produce m/z peaks that are dependent on the pH. At an initial pH of 2.8 the spectra does not exhibit the peak at m/z of 93 as the pH 6 Fe-IHP spectra does. Instead the 2.8 pH spectra exhibits different m/z as detailed previously in Heighton *et al.*, 2008 [18] with the exception of the 163 and 198 m/z clusters. IHP-Fe spectra at high pH exhibit very different spectra than the pH 2.8 and pH 6.0 spectra. IHP-Fe complexes can be expected to be very stable. Khan, 1999 [16] in UV-Vis spectrophotometric studies of IHP-Fe found that dominate species at pH 3.0 and pH 5.0 was Fe_2IHP . This is consistent with the results that we detail in **Table 2** and in the experimental Raman spectra in **Figure 2**. Using the iron in excess of IHP between pH 2.8 and pH 6 is likely governed by a kinetically stable species with proton exchanging sites that are sterically hindered or have variable exchange rates. This in either case would lead to a delay in reaching chemical equilibrium. The use of formic acid in the mobile phase promotes formation of chloride adducts in negative ion ESI

which is the difference in mass between the 163 and 198 m/z cluster [24].

The unexpected development of the 163 and 198 m/z clusters at both pH 2.8 and pH 6.0 provide an analytical benefit that provide insights into the behavior of Fe-IHP couples environmentally. Other siderophores or iron chelating species such as amino carboxylates have been found to provide proton induced enhancement of chelating stability that may be present in IHP-Fe complexes due to the many proton exchanging site on the molecule [25].

4. Conclusions

Significant Raman spectral frequency shifts and changes in spectral intensity were observed as a function of pH for both IHP and P_i solutions allowing for the differentiation of IHP and P_i at several pH points. The ability to simultaneously study IHP and P_i within a single sample may decouple environmentally relevant pathways of fate and transport between the organic and the inorganic phosphorous forms. In addition, the real time analysis of the competitive mineralization processes of IHP and P_i in mineral diverse soil environments is now possible. Although the de-mineralization of P_i is effectively irreversible, de-mineralization of IHP is microbially dependent and microbial populations may increase or decrease in response to specific IHP-mineral complexes. Although, the current lack of sensitivity of normal Raman spectroscopy when applied to IHP and P_i samples makes it of limited use environmentally, incorporation of enhanced Raman techniques will likely solve the sensitivity issue.

ESI-MS enables quantification of IHP iron mineral complex at ppb levels. This method could easily be extended to other matrixes such as manure and aquatic systems potentially impacting human/animal digestive studies and environmental fate and transport issues. The ability to differentiate IHP-iron complexes in diverse soils if coupled with seasonal variations may provide insight into sinks and sources of IHP in the environment. Additionally, extension of the method to other mineral complexes can potentially quantify the amount of mineral or metal associated with IHP at specific pH ranges in environmental and biological systems. ESI-MS and normal Raman spectrometry are not directly comparable due to different detections limits. ESI-MS methods are able to achieve ppb levels of detection while normal Raman spectroscopy is able to detect ppm levels of IHP and IP. The implementation of enhanced Raman methods will potentially improve signal sensitivity and when coupled with Raman mapping, enhanced Raman techniques have the potential to provide ESI-MS level quantization. Future experiments will exploit the ESI-MS IHP-iron complex calibration curve to calibrate enhanced Raman mapping techniques.

REFERENCES

- [1] C. D. Giles, B. J. Cade-Menun and J. E. Hill, "The Inositol Phosphates in Soils and Manures: Abundance, Cycling and Measurement," *Canadian Journal of Soil Science*, Vol. 91, No. 3, 2011, pp. 397-416. [doi:10.4141/cjss09090](https://doi.org/10.4141/cjss09090)
- [2] B. H. Anderson and F. R. Magdoff, "Relative Movement and Soil Fixation of Soluble Organic and Inorganic Phosphorus," *Journal of Environmental Quality*, Vol. 34, No. 6, 2005, pp. 2228-2233. [doi:10.2134/jeq2005.0025](https://doi.org/10.2134/jeq2005.0025)
- [3] E. O. Young and D. S. Ross, "Phosphate Release from Seasonally Flooded Soils," *Journal of Environmental Quality*, Vol. 30, No. 1, 2001, pp. 91-101. [doi:10.2134/jeq2001.30191x](https://doi.org/10.2134/jeq2001.30191x)
- [4] B. L. Turner, M. J. Paphazy, P. M. Haygarth and I. D. McKelvie, "Inositol Phosphates in the Environment," *Philosophical Transactions of the Royal Society B*, Vol. 357, No. 1420, 2002, pp. 449-469. [doi:10.1098/rstb.2001.0837](https://doi.org/10.1098/rstb.2001.0837)
- [5] B. J. Turner and P. M. Haygarth, "Biogeochemistry: Phosphorus Solubilization in Rewetted Soils," *Nature*, Vol. 411, No. 6835, 2001, p. 258. [doi:10.1038/35077146](https://doi.org/10.1038/35077146)
- [6] B. Bar-Yosef, A. C. Chang and S. Vega, "Organic P Transformations Reactions and Transport in Soils Monitored by ^{31}P NMR Spectroscopy," Bard Press, Austin, 1993.
- [7] S. Jayasundera, W. F. Schmidt, J. B. Reeves and T. Dao, "Direct ^{31}P NMR Spectroscopic Measurement of Phosphorous Forms in Dairy Manures," *Journal Food, Agriculture and Environment*, Vol. 3, No. 2, 2005, pp. 335-340.
- [8] J. C. Hansen, B. Cade-Menton and D. S. Srawn, "Phosphorus Speciation in Manure-Amended Alkaline Soils," *Journal of Environmental Quality*, Vol. 33, No. 4, 2004, pp. 1521-1527. [doi:10.2134/jeq2004.1521](https://doi.org/10.2134/jeq2004.1521)
- [9] A. B. Leytem, P. Kwanyuen, P. W. Plumstead, R. O. Mcguire and J. Brake, "Evaluation of Phosphorus Characterization in Broiler Ileal Digesta, Manure, and Litter Samples: ^{31}P -NMR vs. HPLC," *Journal of Environmental Quality*, Vol. 37, No. 2, 2008, pp. 494-500. [doi:10.2134/jeq2007.0134](https://doi.org/10.2134/jeq2007.0134)
- [10] E. T. Champagne, "Effects of pH on Mineral-Phytate, Protein-Mineral-Phytate, and Mineral-Fiber Interactions. Possible Consequences of Atrophic Gastritis on Mineral Bioavailability from High-Fiber Foods," *Journal of the American College of Nutrition*, Vol. 7, No. 6, 1988, pp. 499-508.
- [11] L. Heighton, W. F. Schmidt and R. L. Siefert, "Kinetic and Equilibrium Constants of Phytic Acid, Ferric and Ferrous Phytate Derived from Nuclear Magnetic Resonance Spectroscopy," *Journal of Agriculture and Food Chemistry*, Vol. 56, No. 20, 2008, pp. 9543-9547. [doi:10.1021/jf801465y](https://doi.org/10.1021/jf801465y)
- [12] W. Strumm and J. J. Morgan, "Aquatic Chemistry," John Wiley and Sons Inc., New York, 1996.
- [13] F. M. M. Morel and J. G. Hering, "Principals and Applications of Aquatic Chemistry," John Wiley and Sons Inc., New York, 1993.
- [14] H. Brinch-Pedersen, L. D. Sorensen and P. B. Holm, "Engineering Crop Plants: Getting a Handle on Phosphate," *Trends in Plant Science*, Vol. 7, No. 3, 2002, pp. 118-125. [doi:10.1016/S1360-1385\(01\)02222-1](https://doi.org/10.1016/S1360-1385(01)02222-1)
- [15] J. Pallauf and G. Rimbach, "Nutritional Significance of Phytic Acid and Phytase," *Archives Animal Nutrition*, Vol.

- 50, No. 4, 1997, pp. 301-319.
[doi:10.1080/17450399709386141](https://doi.org/10.1080/17450399709386141)
- [16] S. Y. Khan, "Effects of Dietary Fiber on the Bioavailability of Trace Elements in the Body," Ph.D. Thesis, University of Karachi, Karachi, 1999.
- [17] J. B. Foresman and A. Frisch, "Exploring Chemistry with Electronic Structure Methods," 2nd Edition, Gaussian Inc., Pittsburg, 1996.
- [18] L. Heighton, W. F. Schmidt, C. P. Rice and R. L. Siefert, "Electrospray Ionization Mass Spectroscopy Shows Speciation of Phytate to Be pH Dependent," *Journal of Food, Agriculture and Environment*, Vol. 6, No. 2, 2008, pp. 402-407.
- [19] E. E. Codling, R. L. Chaney and C. L. Mulchi, "Use of Aluminum- and Iron-Rich Residues to Immobilize Phosphorus in Poultry Litter-Amended Soils," *Journal of Environmental Quality*, Vol. 29, No. 6, 2000, pp. 1924-1931.
- [20] Anonymous, "Sigma Plot User's Guide: Part 2—Statistics," Systat Software Inc., 2009.
- [21] V. Barone and M. Cossi, "Quantum Calculation of Molecular Energies and Energy Gradients in Solution by a Conductor Solvent Model," *The Journal of Physical Chemistry A*, Vol. 102, No. 11, 1998, pp. 1995-2001.
[doi:10.1021/jp9716997](https://doi.org/10.1021/jp9716997)
- [22] V. Barone, M. Cossi and J. Tomasi, "Geometry Optimization of Molecular Structures in Solution by the Polarizable Continuum Model," *Journal of Computational Chemistry*, Vol. 19, No. 4, 1998, pp. 404-417.
[doi:10.1002/\(SICI\)1096-987X\(199803\)19:4<404::AID-JCC3>3.0.CO;2-W](https://doi.org/10.1002/(SICI)1096-987X(199803)19:4<404::AID-JCC3>3.0.CO;2-W)
- [23] M. Cossi, N. Rega, G. Scalamani and V. Barone, "Energies, Structures, and Electronic Properties of Molecules in Solution with the C-PCM Solvation Model," *Journal of Computational Chemistry*, Vol. 24, No. 6, 2003, pp. 669-681. [doi:10.1002/jcc.10189](https://doi.org/10.1002/jcc.10189)
- [24] J. Zhu and R. B. Cole, "Formation and Decompositions of Chloride Adduct Ions, $[M + Cl]^-$, in Negative Ion Electrospray Ionization Mass Spectrometry," *Journal American Society for Mass Spectrometry*, Vol. 11, No. 11, 2000, pp. 932-941. [doi:10.1016/S1044-0305\(00\)00164-1](https://doi.org/10.1016/S1044-0305(00)00164-1)
- [25] N. von Wiren, H. Khodr and R. C. Hider, "Hydroxylated Phytosiderophore Species Possess an Enhanced Chelate Stability and Affinity for Iron (III)," *Plant Physiology*, Vol. 124, No. 3, 2000, pp. 1149-1157.
[doi:10.1104/pp.124.3.1149](https://doi.org/10.1104/pp.124.3.1149)